arXiv:1611.09063v1 [stat.ME] 28 Nov 2016

Estimating viral covariances using Bayesian multivariate conditional autoregressive models.

Colette Mair*[1,2], Sema Nickbakhsh[2], Richard Reeve[1,2], Jim McMenamin[3], Arlene Reynolds[3], Rory Gunson[4], Pablo R Murcia[2], and Louise Matthews[1,2]

[1]Boyd Orr Centre for Population and Ecosystem Health, Institute of Biodiversity, Animal Health and Comparative Medicine, College of Medical, Veterinary and Life Sciences, University of Glasgow, Glasgow, UK.
[2]MRC-University of Glasgow Centre for Virus Research, Institute of Infection, Immunity and Inflammation, College of Medical, Veterinary and Life Sciences, University of Glasgow, Glasgow, UK.
[3]Health Protection Scotland, NHS National Services Scotland, Glasgow, UK.
[4]West of Scotland Specialist Virology Centre, NHS Greater Glasgow and Clyde, Glasgow, UK.

November 29, 2016

Abstract

Bayesian disease mapping methods are typically used to estimate spatial patterns of disease risk through conditional autoregressive priors on spatial parameters. Recent extensions capture temporal autocorrelations as well as data from multiple diseases. We integrated disease surveillance approaches and Bayesian multivariate disease mapping to develop a framework for modelling viral infection time series data that enables us to estimate between virus covariances and identify significant seasonal associations between multiple viruses. We applied this framework to monthly counts of respiratory viruses (adenovirus [AdV], coronavirus [Cov], human metapneumovirus [MPV], influenza B virus [IBV] and respiratory syncytial virus [RSV]) detected by routine diagnostics at the West of Scotland Specialist Virology Center (WoSSVC) between 2005 and 2013. We found a significant positive covariance between RSV & MPV and negative covariances between IBV & AdV, IBV & MPV and Cov & MPV indicating that biological or behavioural factors may generate interactions between certain virus pairs.

1 Introduction

Public health policy and preparedness for disease outbreaks, epidemics and pandemics depend on mathematical and statistical analysis of infectious disease data.

*Colette.Mair@glasgow.ac.uk

Statistical methods for epidemic detection range from regression techniques to time series analyses [1]. An epidemic may be inferred if a predicted incidence rate exceeds a pre-determined threshold value. In additional to epidemic detection, seasonality can be inferred parametrically, using trigonometry functions, or non-parametrically, using regression based techniques [2].

Modelling time series count data from infectious diseases should necessarily capture both seasonality and other temporal dependencies, such as disease outbreaks [3]. One approach is to view infectious disease count data as the sum of two components. The first parametric component describes endemic seasonal patterns and the second non-parametric component describes possible disease epidemics [4]. This framework captures both within- and between-year autocorrelations typical of monthly time series data for infectious diseases, such as influenza, which are subject to seasonal outbreaks and epidemics [5, 6].

In addition to temporal data, spatial data is often utilized to analyse local or regional variation in disease incidences, such as localized detection of outbreaks, using spatial-temporal regression models [7, 8].

Disease mapping models are a class of spatio-temporal regression model and have received much attention in recent years [9] for the analysis of spatial distributions of incidence data routinely collected by public health bodies [10]. Under this framework the observed count of a disease, or pathogen, at a given location is modelled in terms of the true unknown relative risk of that pathogen at that location (to be estimated) and a pre-determined expected number of cases [1] (fully specified and fixed). The expected number of cases may reflect global counts or region specific counts standardised for demographics such as age and gender taken from a known reference population [11]. The estimated relative risk describes the risk of infection in relation to that expected. These models are typically used to estimate spatial patterns of a disease risk over some geographical region with several models proposed to capture spatial autocorrelations [12, 13]. However, extensions have been made to include temporal data [14, 12] and space-time interactions [15, 16]. Space-time analyses simultaneously examines persistent temporal patterns and identify unusual patterns such as outbreaks [17, 6].

In the case of multiple infections, relative risks can be estimated using multivariate disease mapping methodology [18]. One motivation for modelling diseases multivariately, as opposed to a series of univariate models, is to assess disease similarities in geographical or temporal distributions [19, 20, 21]. More precisely these models may be used to estimate between-disease dependencies through a covariance matrix by imposing a multivariate normal structure on disease risks [22, 23]. Testing the off-diagonal elements of this covariance matrix can be used to infer significant pairwise spatial or temporal associations between disease risks [24].

Respiratory infections are associated with a variety of health outcomes from mild cold to severe illness and are caused by multiple pathogens of which viruses are believed to be the most common agent [25]. Diagnostic tests routinely used in the UK healthcare system permit simultaneous detection of multiple viruses and are used for monitoring respiratory viruses as part of national surveillance programs [26]. As respiratory viruses infect the same anatomical regions (i.e. the respiratory tract) it is possible that interactions between viruses affect infection risk patterns. Consequently, inference about infection risk should be carried out with consideration to the community of viruses as a whole and not on the

basis of individual viruses [1, 27]. The existence of dependencies between viruses could mean that control measures against one virus could influence the infection incidence of the another virus [28]. Thus, inferring dependencies between viruses could influence public health planning and preparedness and have implications for vaccination strategies.

The aim of this paper was to develop a framework for inferring dependencies between multiple respiratory viruses by estimating pairwise virus covariances. The adopted method accounts for potential demographic risk factors such as age, gender and disease severity (estimated by hospital or general practice submission) using time series data generated by routine virological diagnostics for five co-circulating viruses in the UK [29]. The method employed combines disease surveillance models [4] with multivariate disease mapping methodology [10, 30].

2 Respiratory virus infection time series data

Our dataset comprises 60,971 clinical samples virologically tested for respiratory viruses by the West of Scotland Specialist Virology Center (WoSSVC) for Greater Glasgow and Clyde Health Board between January 2005 and December 2013. Each sample was tested by multiplex real-time RT-PCR and test results (virus positive or negative) were available for five groups of respiratory viruses: adenovirus (AdV); coronavirus (CoV); human metapneumovirus (MPV); influenza B virus (IBV); and respiratory syncytial virus (RSV) [26]. Sampling date, patient age, patient gender, the sample origin (hospital or general practice submission that we used as a proxy for infection severity) were recorded. Multiple samples from the same patient received within a 30-day period were aggregated into a single episode of respiratory illness. The 60,971 clinical samples corresponded to 36,157 patient episodes. A patient was considered virus-positive during an episode if at least one clinical sample was positive during the 30-day window.

In total, 35% of patients tested positive for at least one virus and detection was most prevalent in children aged between 1 and 5 years [29]. Detection of at least one virus in a given clinical sample was most common in December and least common in August, however. We observed differing patterns between the five viruses (Figure 1, black lines); IBV, RSV and CoV were more prevalent in winter whereas AdV amd MPV were less common on average, with a slight increased prevalence in spring [29].

3 Modelling disease surveillance data

Infectious disease data have previously been modelled using Poisson or negative binomial models with two components: an endemic and an epidemic component [31, 4, 7]. These types of models assume the observed count of a disease at a given time point, Y_t, can be decomposed additively into an endemic process, accounting for seasonality, and an epidemic process, accounting for temporal dependencies beyond seasonality such as outbreaks [4, 8].

The epidemic component is modelled autoregessively on the number of cases at the previous time point Y_{t-1}. It can be extended to incorporate spatial data or cases of multiple diseases by modelling this component as a weighted sum

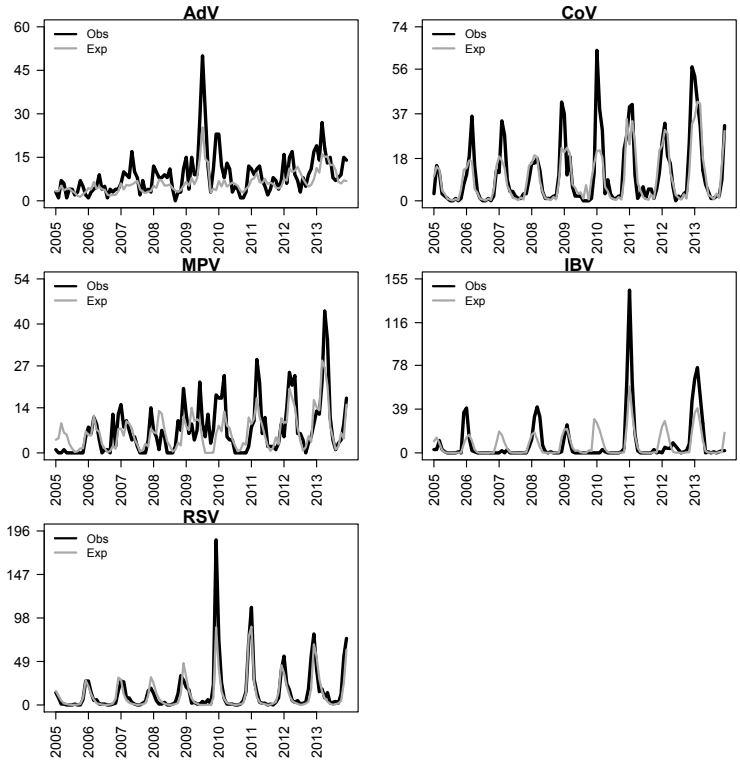

Figure 1: Observed (Obs) and expected (Exp) counts of the five groups of respiratory viruses between 2005 and 2013 (black and grey lines respectively). Expected counts were estimated as described in main text.

of cases from pre-defined 'neighbouring' locations or the number of cases of a related disease [7]. For instance, a disease count from a specific location and time can be modelled in terms of the count from the previous time point, disease counts from neighbouring geographical locations and some residual variation [6]. This approach is similar to modelling spatial autocorrelations in a disease mapping context.

The endemic component captures seasonality. Sinusoidal waves are typically used to model seasonal patterns in time series data [31]. However, non-parametric regression based methods offer an alternative to this type of parameter-driven model [2].

Comparing observed disease counts both spatially and temporally to those expected, given a range of covariates, can provide evidence of potential disease outbreaks [32]. Expected counts represent standardised disease rates [10]. By comparing expected and observed cases of a disease an excess risk within an area or at a specific time point can be identified [30].

The methodology referenced in this section was primarily designed to model epidemic events from time series data. Although this differs from the main objective of this paper, our adopted methodology, described in the following section, makes comparable assumptions and captures similar characteristics of surveillance data from multiple viruses.

4 Bayesian multivariate conditional autoregressive models

Conditional autoregressive models are extensively used in the analysis of spatial data to model the relative risk of a virus or more generally a disease [30, 33]. The class of Bayesian model typically used in this context is given by

$$\begin{aligned} Y_i|E_i, RR_i &\sim \text{Poisson}(E_i RR_i) \\ \log(RR_i) &= \alpha + \phi_i \end{aligned} \qquad \text{(Model 1)}$$

where Y_i, E_i and RR_i are the observed count, expected count and relative risk at location i [13]. The expected number of cases E_i are usually based upon some standard population [10]. Standardisation of this kind can require adjustment for several factors such as age and sex. When individual data are available, logistic regression can be used to estimate the probability of testing positive for a virus at a given location or time-frame through a set of explanatory variables [11]. Parameter α is an intercept term and parameters $\phi = \{\phi_1, \ldots, \phi_I\}$ are random effects commonly modelled through conditional autoregressive (CAR) prior distributions. The joint distribution can be written as [22]

$$\phi \quad \sim \quad \text{MVN}(0, \Omega^{-1}).$$

The precision matrix Ω can take a variety of forms to capture spatial autocorrelations. It is defined in terms of a proximity matrix W with $w_{ii} = 0$ and $w_{jk} = 1$ $(j \neq k)$ if locations j and k are neighbours [34].

Model 1 has been extended to incorporate temporal trends:

$$\begin{aligned} Y_{it}|E_{it}, RR_{it} &\sim \text{Poisson}(E_{it} RR_{it}) \\ \log(RR_{it}) &= \alpha + \phi_{it} \end{aligned} \qquad \text{(Model 2)}$$

where Y_{it}, E_{it} and RR_{it} are the observed count, expected count and relative risk at location i and time t [15, 14, 16]. Temporal correlations can be induced through the condition expectation of $\phi_{.t}|\phi_{.t-1}$:

$$\phi_{.t}|\phi_{.t-1} \quad \sim \quad \text{MVN}(s\phi_{.t-1}, \Omega^{-1})$$

with s a smoothing parameter controlling the amount of temporal autocorrelation [15].

Furthermore, Model 1 can be extended to incorporate multiple types of viral infection:

$$\begin{aligned} Y_{iv}|E_{iv}, RR_{iv} &\sim \text{Poisson}(E_{iv} RR_{iv}) \\ \log(RR_{iv}) &= \alpha_v + \phi_{iv} \end{aligned} \qquad \text{(Model 3)}$$

where Y_{iv}, E_{iv} and RR_{iv} are the observed count, expected count and relative risk of virus v at location i and α_v a virus specific intercept term. CAR priors used to jointly model ϕ can be extended to a multivariate CAR prior (MCAR) by incorporating a between virus covariance matrix Λ^{-1} of dimension $V \times V$ (where V is the total number of diseases):

$$\phi \quad \sim \quad \text{MVN}(0, [\Omega \otimes \Lambda]^{-1}).$$

In this case, $\phi = \{\phi_{.1}, \ldots, \phi_{.V}\}$ and $\phi_{iv} = \{\phi_{1v}, \ldots, \phi_{Iv}\}$ [35, 24].

4.1 A multivariate spatial-temporal conditional autoregressive model

By combining Model 2 and Model 3, we can model spatial-temporal count data for multiple viruses simultaneously:

$$\begin{aligned} Y_{itv}|E_{itv}, RR_{itv} &\sim \text{Poisson}(E_{itv}RR_{itv}) \\ \log(RR_{itv}) &= \alpha_v + \phi_{itv} \end{aligned} \qquad \text{(Model 4)}$$

where Y_{itv}, E_{itv} and RR_{itv} are the observed count, expected count and relative risk of virus v at location i time t and α_v a virus specific intercept term. Now, let $\phi_{.t.} = \{\phi_{.t1}, \ldots, \phi_{.tV}\}$ and $\phi_{.tv} = \{\phi_{1tv}, \ldots, \phi_{Itv}\}$. We model the conditional distribution of $\phi_{.t.}|\phi_{.t-1.}$ as

$$\phi_{.t.}|\phi_{.t-1.} \quad \sim \quad \text{MVN}(s_v\phi_{.t-1.}, [\Omega \otimes \Lambda]^{-1})$$

with s_v a virus specific temporal autocorrelation smoothing parameter.

4.2 Modelling multivariate time series data

Model 4 can be adapted to model time series data from multiple viruses. In this setting, we model the observed count of virus v in the mth month of year t, Y_{mtv}, in terms of the expected count E_{mtv} and relative risk RR_{mtv}:

$$\begin{aligned} Y_{mtv}|E_{mtv}, RR_{mtv} &\sim \text{Poisson}(E_{mtv}RR_{mtv}) \\ \log(RR_{mtv}) &= \alpha_v + \phi_{mtv} \end{aligned} \qquad \text{(Model 5)}$$

with α_v a virus specific intercept term and ϕ_{mtv} a random effect modelled through a conditional MCAR distribution

$$\phi_{.t.}|\phi_{.t-1.} \quad \sim \quad \text{MVN}(s_v\phi_{.t-1.}, [\Omega \otimes \Lambda]^{-1}).$$

The conditional expectation of $\phi_{.t.}$ depends on the previous year $\phi_{.t-1.}$ and monthly autocorrelations are captured through 12×12 matrix Ω. By allowing dependencies between neighbouring months, we can account for seasonality in viral infection frequencies. The between virus covariance matrix Λ^{-1} captures dependencies between viral relative risks in terms of monthly trends.

This parameterisation of a MCAR model captures both the seasonal trends of each virus (an endemic component) and additional temporal trends (an epidemic component) comparable to other virus surveillance data models [4, 6, 3].

4.3 MCAR prior specification

The MCAR distribution used to model random seasonal-temporal effects in Model 5 required specification of precision matrix Ω and estimation of matrix Λ. Matrix Ω captured seasonal trends in terms of monthly dependencies through a proximity matrix W. Matrix W was defined as a 12×12 matrix with zero diagonal elements and off-diagonal elements $\in \{0, 1\}$:

$$W = \begin{pmatrix} 0 & 1 & 1 & 1 & 0 & 0 & 0 & 0 & 0 & 1 & 1 & 1 \\ 1 & 0 & 1 & 1 & 1 & 0 & 0 & 0 & 0 & 0 & 1 & 1 \\ 1 & 1 & 0 & 1 & 1 & 1 & 0 & 0 & 0 & 0 & 0 & 1 \\ 1 & 1 & 1 & 0 & 1 & 1 & 1 & 0 & 0 & 0 & 0 & 0 \\ 0 & 1 & 1 & 1 & 0 & 1 & 1 & 1 & 0 & 0 & 0 & 0 \\ 0 & 0 & 1 & 1 & 1 & 0 & 1 & 1 & 1 & 0 & 0 & 0 \\ 0 & 0 & 0 & 1 & 1 & 1 & 0 & 1 & 1 & 1 & 0 & 0 \\ 0 & 0 & 0 & 0 & 1 & 1 & 1 & 0 & 1 & 1 & 1 & 0 \\ 0 & 0 & 0 & 0 & 0 & 1 & 1 & 1 & 0 & 1 & 1 & 1 \\ 1 & 0 & 0 & 0 & 0 & 0 & 1 & 1 & 1 & 0 & 1 & 1 \\ 1 & 1 & 0 & 0 & 0 & 0 & 0 & 1 & 1 & 1 & 0 & 1 \\ 1 & 1 & 1 & 0 & 0 & 0 & 0 & 0 & 1 & 1 & 1 & 0 \end{pmatrix}.$$

We set

$$\Omega \quad = \quad D - \lambda W$$

where λ was a smoothing parameter and D a 12×12 diagonal matrix with the ith entry equal to the total number of 'neighbouring' months to month i [35]. We note that this formation can easily be extended [34]. For instance, allowing disease specific smoothing parameters [35].

Wishart priors can be used for unstructured covariances matrices such as Λ [23], however, we employed a modified Cholesky decomposition to estimate covariance matrix Λ^{-1}:

$$\Lambda^{-1} \quad = \quad \Sigma\Gamma\Gamma^T\Sigma$$

where Σ was a diagonal matrix with elements proportional to viral standard deviations and Γ a lower triangular matrix relating to viral correlations [36]. This parameterisation ensured the positive-definiteness of Λ^{-1}, although we note that other parameterisations are available [37].

4.4 Full model

Let Y_{mtv} denote the observed count of virus v during the mth month of year t, V the total number of viruses and T the number of years. Following Model 5, we modelled Y_{mtv} in terms of the expected count E_{mtv} and relative risk RR_{mtv} and used a Cholesky decomposition to estimate covariance matrix Λ^{-1} [38] (Figure 2).

This model was implemented in jags [39] using the R2jags package [40] in R [41]. All results are averaged across five independent chains. In each chain, we took the 100th draw across 500,000 iterations after a burn-in period of 300,000 iterations. Our R code used to model these data and an example of simulated are available upon request to first author.

5 Simulation Studies

5.1 Three virus example

We first present an analysis of simulated data for three viruses. We simulated monthly virus counts over a four year period and set a sample size of 200 tests for each virus in each month with the exception of virus 2 in the third year where we set a sample size of 1500 tests between April and September. We specified uniform probabilities of a test being positive for each virus. Probabilities of being positive for viruses 1 and 2 were between (0.1, 0.22) from October to January and between (0.005, 0.1) from February to September. The probability of being positive for virus 3 was between (0.0001, 0.2) throughout the year. For each virus, at each time point, the expected count was set to be the probability of that virus multiplied by the number of tests. Viruses 1 and 2 peak during autumn and winter of each year whereas virus 3 remains at low frequencies throughout the year (Figure 3). There was a dramatic increase in virus 2 during the summer of year 3. Random effects ϕ were drawn from multivariate normal distributions with yearly smoothing parameters and monthly

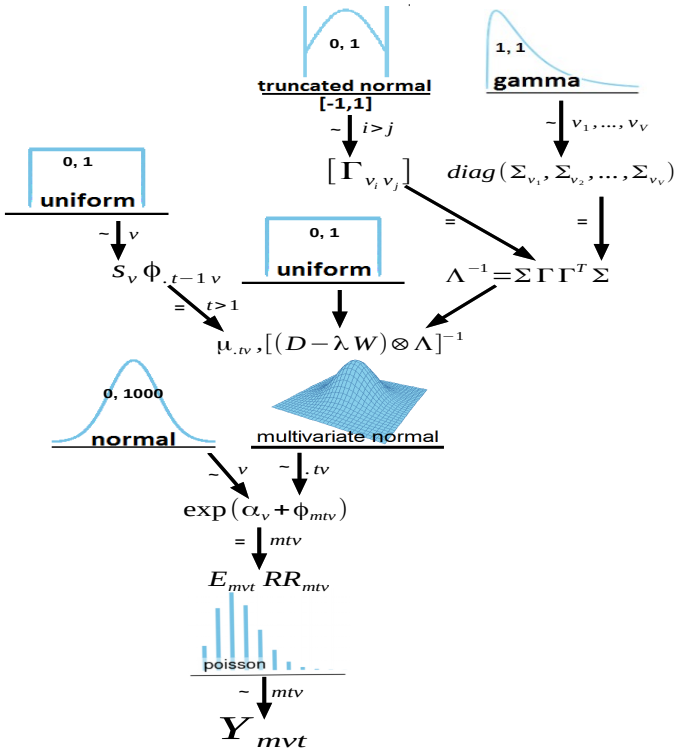

Figure 2: Diagram of full model used to estimate pairwise relative risk covariances. The diagram should be read from the bottom (starting with Y_{mtv}) to the top. All prior choices have been fully specified. Numbers indicate hyperparameter choices, for instance, mean and variance in the normal distribution, lower and upper bound in the uniform distributions and shape and rate in the gamma distribution.

smoothing parameter (s_1, s_2, s_3 and λ) set as 0.5. Matrices W and D were defined as described in the previous section. Lastly we set $\alpha_1 = \alpha_2 = 1$ and $\alpha_3 = -1$.

The primary interest was in estimating the covariance matrix Λ^{-1}. Virus 1 and virus 2 were positively correlated and both viruses were independent of virus 3 (Table 1, fixed values). The full model correctly identified a significantly positive covariance between virus 1 and virus 2 and non-significant covariances between virus 1 and virus 3 and between virus 2 and virus 3 (table 1).

By taking the absolute difference between the true relative risks and the estimated relative risks, d, we found the estimated pattern of relative risks across the time frame of this simulation followed closely to the true relative risks (Figure 4).

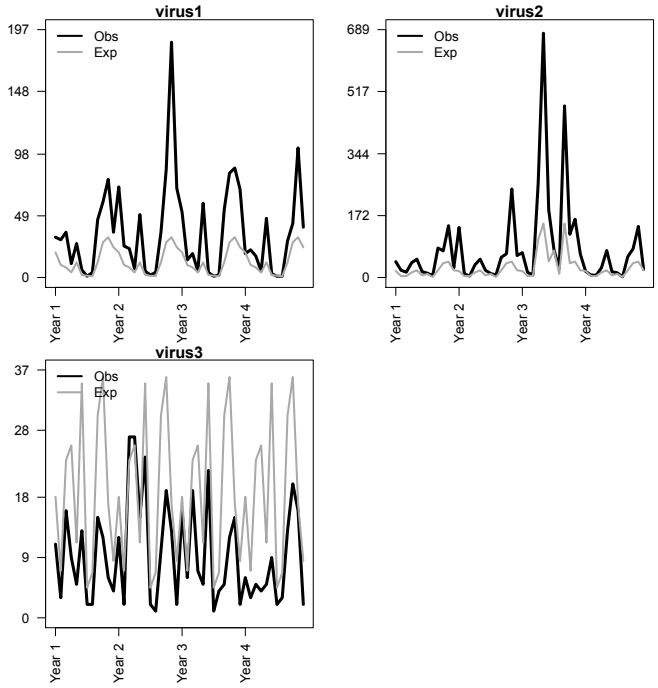

Figure 3: Simulated observed and expected virus counts from three viruses over four years.

5.2 Five virus example

In order to illustrate the accuracy of the full model in estimating virus correlations, we simulated data from five viruses over a 15 year period (Figure 5) with

$$\Lambda^{-1} = \begin{pmatrix} 1 & 0.5 & 0 & 0 & 0 \\ 0.5 & 1 & 0 & 0 & 0 \\ 0 & 0 & 1 & 0 & 0 \\ 0 & 0 & 0 & 1 & -0.5 \\ 0 & 0 & 0 & -0.5 & 1 \end{pmatrix}.$$

Virus 1 and virus 2 were positively correlated, virus 4 and virus 5 were negatively correlated and virus 3 circulated independently. Counts from the

parameter	true value	95% credible interval
$\Lambda^{-1}_{1,1}$	1	$(0.39, 1.17)$
$\Lambda^{-1}_{1,2}$	0.5	$(0.29, 0.81)$
$\Lambda^{-1}_{1,3}$	0	$(-0.15, 0.58)$
$\Lambda^{-1}_{2,2}$	1	$(0.53, 1.41)$
$\Lambda^{-1}_{2,3}$	0	$(-0.19, 0.61)$
$\Lambda^{-1}_{3,3}$	1	$(0.29, 1.49)$

Table 1: True values of matrix Λ from simulation study and estimated 95% credible intervals from full model.

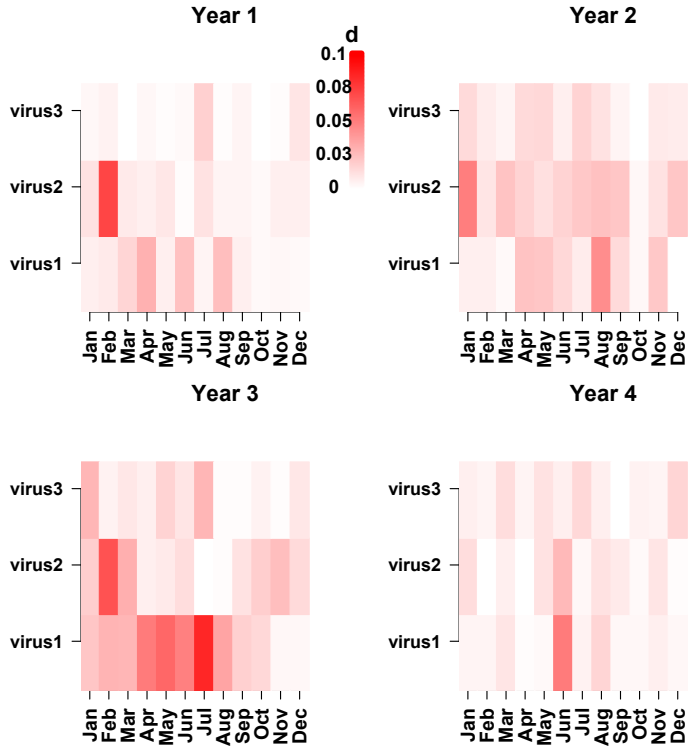

Figure 4: Absolute difference d between the true relative risks used in simulated study and the estimated relative risk from full model.

first three viruses were simulated under identical conditions to those described in the three viruses example. The probability of being positive for virus 4 was between (0.2, 0.3) in the first three months and the last two months. In the remaining months, the probability of being positive for virus 4 was between (0.000001, 0.0003). The probability of being positive for virus 5 was between (0.000001, 0.0003) in the first three months and the last two months and between (0.2, 0.3) in the remaining months.

We initially estimated Λ^{-1} using only the first year of data. We then combined the first two years of data to estimated Λ^{-1}. This process was repeated, adding the current year's data at each iteration, until all fifteen years of data were combined to estimate Λ^{-1}.

For each pair of viruses, we tested the significance of the corresponding covariance parameter and therefore applied a multiple comparison. We choose to control the false discovery rate (the expected proportion of falsely rejected hypotheses amongst those rejected) at rate of 0.05 [42].

Using data from the first three years, we estimated non-significant correlations between all pairs of viruses (Figure 6, year 1, year 2 and year 3). Using data from four years onwards, we found varying degrees of significance in the correlation between virus 1 and virus 2, $\Lambda^{-1}_{1,2}$, virus 1 and virus 4, $\Lambda^{-1}_{1,4}$, and virus 4 and virus 5, $\Lambda^{-1}_{4,5}$ (Figure 6, year 4 onwards). Following the multiple comparison correction, we found significant correlations between virus 1 and

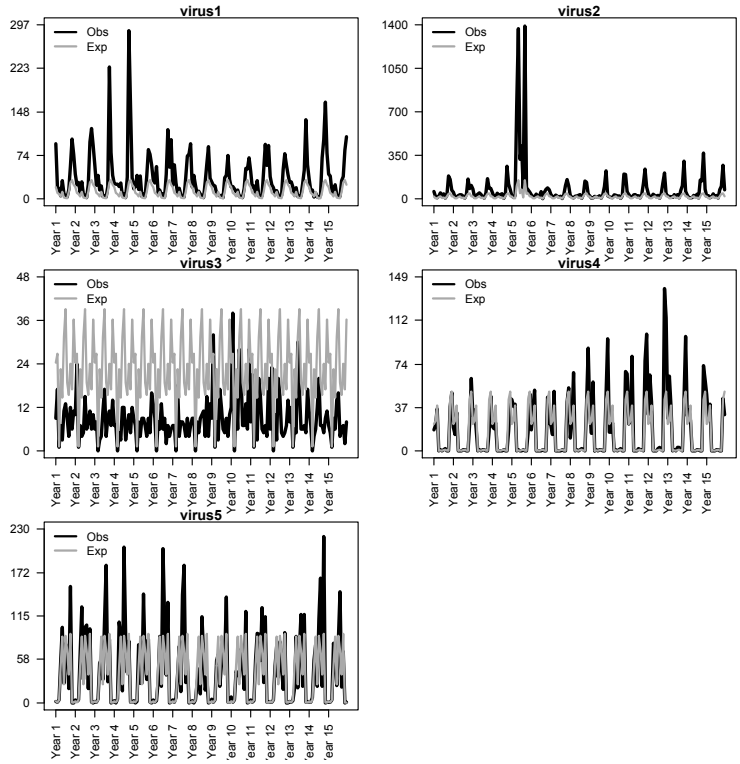

Figure 5: Simulated observed and expected virus counts from five viruses over fifteen years.

virus 2, $\Lambda_{1,2}^{-1}$ and virus 4 and virus 5, $\Lambda_{4,5}^{-1}$ from year 12 onwards (Figure 6, thick navy and purple lines).

6 Application to virological diagnostic data

We applied Model 5 to the multivariate respiratory virus data with particular interest in estimating significant covariances in seasonal trends between viruses (matrix Λ^{-1}).

6.1 Expected counts

Expected counts were estimated using a series of logistic regressions. For month m in year t, the log odds of virus v, logit_{mtv}, was estimated through fixed effects age, sex and severity and a patient random effect:

$$\begin{aligned}\widehat{\text{logit}}_{mtv} = \hat{\alpha} + \hat{\beta}_{1,sex} + \hat{\beta}_2 age + \hat{\beta}_{3,origin} \\ + \hat{\gamma}_{Patient\cdot}\end{aligned} \qquad \text{(Model 6)}$$

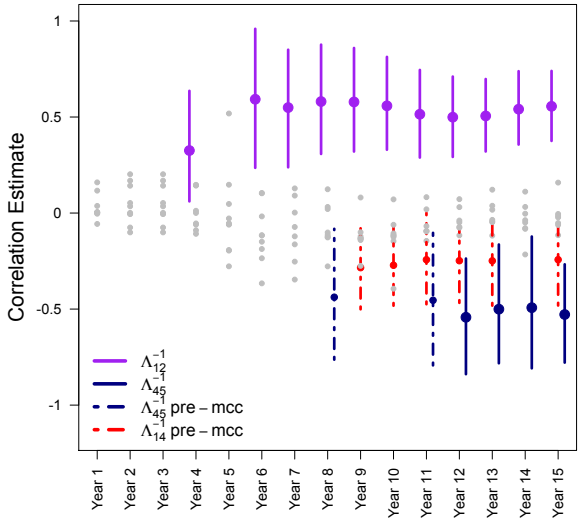

Figure 6: Estimated correlation parameters significantly different from zero using data from year 1 through to year 15. Grey dots show point estimates of all correlation parameters at each time point. Solid lines show parameters significantly different from zero once multiple comparison correction (mcc) was applied. Dotted lines show parameters only significantly different from zero before multiple comparison correction (pre-mcc).

For each age (a), sex (s) and sample origin (l) combination, a standardised logit $\widehat{\text{slogit}}_{mtv}$ was estimated as

$$\widehat{\text{slogit}}_{mtv} = \sum_{a,s,l} \frac{N_{asl}\widehat{\text{logit}}_{mtv_{asl}}}{N_{mtv}},$$

where N_{asl} was the number of observations in that age, sex and sample origin combination from the subset of data used, N_{mtv} the number of observations for virus v in month m and year t and $\widehat{\text{logit}}_{mtv_{asl}}$ the log odds of having a virus for sex s, age a and sample origin l estimated from Model 6 . The standardised probability of having virus v was estimated as

$$\widehat{\text{p}}_{mtv} = \frac{\exp(\widehat{\text{slogit}}_{mtv})}{1+\exp(\widehat{\text{slogit}}_{mtv})}.$$

The expected count for virus v in month m and year t was then estimated as

$$E_{mtv} = N_{mtv}\widehat{\text{p}}_{mtv}$$

(Figure 1, grey lines).

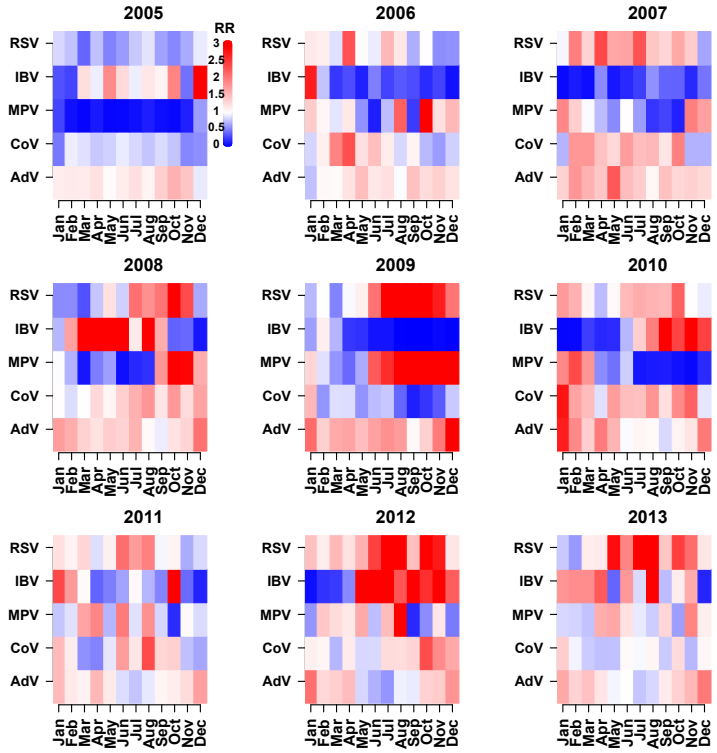

Figure 7: Estimated relative risks (RR) of adenovirus (AdV), coronavirus (Cov), human metapneumovirus (MPV), influenza B virus (IBV) and human Respiratory syncytial virus (RSV) 2005 and 2013.

6.2 Estimating RR and Λ^{-1}

We found a positive covariance between RSV & MPV (adjusted p-value = 0.01) and negative covariances between IBV & AdV (adjusted p-value = 0.049), IBV & MPV (adjusted p-value = 0.049) and Cov & MPV (adjusted p-value = 0.049) (Table 2).

The relative risk of AdV infection remained relatively high between 2005 to 2010 but decreased during the summer months of 2011, 2012 and 2013 (Figure 7, AdV). We found an increased relative risk of IBV infection during alternate winter periods (Figure 7, IBV, winter months of 2005/2006, 2010/2011 and 2012/2013). During the second half of 2009, we found a heightened risk of RSV and MPV infections. More generally, the relative risk of RSV infection peaked during late summer through to autumn from 2008 onwards whereas the risk of MPV infection shifted from winter, between 2005 and 2008, to summer, from 2011 onwards (Figure 7, RSV and MPV).

7 Discussion

We have presented a method of estimating covariances between respiratory virus infections using time series data. Our analyses were based on routine diagnos-

	Adv	Cov	MPV	IBV	RSV
Adv	1				
Cov	(-0.27, 0.45)	1			
MPV	(-0.35, 0.22)	**(-0.66, -0.11)**	1		
IBV	**(-0.67, -0.16)**	(-0.23, 0.45)	**(-0.66, -0.13)**	1	
RSV	(-0.37, 0.29)	(-0.28, 0.32)	**(0.32, 0.71)**	(-0.51, 0.05)	1

Table 2: Posterior density interval estimates of correlations between adenovirus (AdV), coronavirus (Cov), human metapneumovirus (MPV), influenza B virus (IBV) and respiratory syncytial virus (RSV).

tic testing of clinical specimens of patients attending primary and secondary health care services between 2005 and 2013. Observed counts were decomposed into expected counts and relative risks. Expected counts were estimated using a series of logistic regressions using age, gender and testing origin (GP or hospital) to estimate the probability of infection of a given respiratory virus [11]. The monthly risks of detecting a virus were estimated relative to the estimated expected counts through random effects that capture temporal autocorrelations [30]. We assumed that yearly viral counts depended on the previous years counts [15]. Monthly autocorrelations were modelled in terms of a proximity matrix W [24] with counts in a particular month dependent on counts from the previous and proceeding three months although other configurations are valid.

Our assumptions are typical of statistical modelling of diseases time series data [4], capturing both within and between year viral infection incidences. However, by analysing the data within a disease mapping framework, we were able to directly estimate correlations between multiple viruses.

Simulation studies of three and five viruses validated the application of Bayesian disease mapping to longitudinal infectious disease data.

We found positive covariances between respiratory syncytial virus [RSV] and human metapneumovirus [MPV] and negative covariances between influenza B virus [IBV], adenovirus [AdV] and human metapneumovirus [MPV] and between human metapneumovirus [MPV] and coronavirus [Cov] (Figure 7 and Table 2). Viral interactions between common respiratory viruses have been postulated by several studies, using observational methods or individual regression based models, with particular interest in influenza A [27, 43]. Our analysis offers an alternative method to formally assess associations between multiple viruses. This method takes into account confounding variables, such as age and gender, and estimates the relative risk of each virus and pairwise covariances between viruses in terms of temporal autocorrelation.

Acknowledgments

This work was funded by the Medical Research Council of the United Kingdom (Grant number MC_UU_12014/9). We are grateful for support from National Science Foundation DEB1216040, BBSRC grants BB/K01126X/1, BB/L004070/1, BB/L018926/1, BB/L018926/1, BB/N013336/1, BB/L004828/1, BB/H009302/1, BB/H009175/1, the Foods Standards Agency FS101055 and the Scottish Government Rural and Environment Science and Analytical Services Division, as part of the Centre of Expertise on Animal Disease Outbreaks (EPIC). We thank Paul Johnson for his helpful comments on the manuscript.

References

[1] Steffen U, Farrington C, Garthwaite P, Robertson C, Andrews N. Statistical methods for the prospective detection of infectious disease outbreaks: a review. J R Stat Soc Ser A Stat Soc. 2012;175:49–82.

[2] Naumova E, Jagai J, Matyas B, Jr ADM, MacNeill I, Griffiths J. Seasonality in six enterically transmitted diseases and ambient temperature. Epidemiol Infect. 2007;135:281–292.

[3] Conesa D, Martinez-Beneito M, Amoros R, Lopez-Quilez A. Bayesian hierarchical Poisson models with a hidden Markov structure for the detection of influenza epidemic outbreaks. Stat Methods Med Res. 2015;24:206–223.

[4] Knorr-Held L, Hofmann M, Hohle M. A two-component model for counts of infectious diseases. Biostatistics. 2006;7:422–437.

[5] Mugglin A, Cressie N, Gemmell I. Hierarchical statistical modelling of influenza epidemic dynamics in space and time. Stat Med. 2002;21:2703–2721.

[6] M LKH, Paul. Modeling seasonality in space-time infectious disease surveillance data. Biom J. 2012;54:824–843.

[7] Paul M, Knorr-Held L, Toschke A. Multivariate modelling of infectious disease surveillance data. Stat Med. 2008;27:6250–6267.

[8] Knorr-Held L, Richardson S. A hierarchical model for space-time surveillance data on meningococcal disease incidence. J R Stat Soc Ser C Appl Stat. 2003;52:169–183.

[9] AB Lawson DL, MacNab Y. Editorial. Stat Methods Med Res. 2016;25(4):1079.

[10] Lawson A, Williams F. An introductory Guide to Disease Mapping. UK: John Wiley & Sons, Ldt; 2001.

[11] Roalfe AK HR, S W. Standardisation of rates using logistic regression: a comparison with the direct method. BMC Health Serv Res. 2008;8:1–7.

[12] Knorr-Held L, Besag J. Modelling Risk from a Disease in Time and Space. Stat Med. 1998;17:2045–2060.

[13] Lee D. A comparison of conditional autoregressive models used in Bayesian disease mapping. Spat Spatiotemporal Epidemiol. 2011;2:79–89.

[14] Robertson C, Nelson T, MacNab Y, Lawson A. Review of methods for space-time disease surveillance. Spat Spatiotemporal Epidemiol. 2010;1:105–116.

[15] Rushworth A, Lee D, Mitchell R. A spatial-temporal model for estimating the long-term effects of air pollution on respiratory hospital admissions in Greater London. Spat Spatiotemporal Epidemiol. 2014;10:29–38.

[16] Knorr-Held L. Bayesian Modelling of Inseparable Space-Time Variation in Disease Risk. Stat Med. 2000;19:2555–2567.

[17] Richardson S, Abellan J, Best N. Bayesian spatio-temporal analysis of joint patterns of male and female lung cancer risks in Yorkshire (UK). Stat Methods Med Res. 2006;15:385–407.

[18] Manda S, Feltbower R, Gilthorpe M. Review and empirical comparison of joint mapping of multiple diseases. South Afr J Infect Dis. 2012;27:169–182.

[19] Dabney A, Wakefield J. Issues in the mapping of two diseases. Stat Methods Med Res. 2005;14:83–112.

[20] Held L, Natario I, Fenton S, Rue H, Nikolaus B. Towards joint disease mapping. Stat Methods Med Res. 2005;14:61–82.

[21] Downing A, Forman D, Gilthorpe M, Edwards K, Manda S. Joint disease mapping using six cancers in the Yorkshire region of England. Int J Health Geogr. 2008;7:1–14.

[22] Martinez-Beneito M. A general modelling framework for multivariate disease mapping. Biometrika. 2013;100:539–553.

[23] YC M. Mapping disability-adjusted life years: A Bayesain hierarchical model framework for burden of disease and injury assessment. Stat Med. 2007;26:4746–4769.

[24] MacNab Y. On Bayesian shared component disease mapping and ecological regression with errors in covariates. Stat Med. 2010;29:1239–1249.

[25] Englund J, Feuchtinger T, Ljungman P. Viral Infections in Immunocompromised Patients. Biol Blood Marrow Transplant. 2011;17:S2–S5.

[26] Gunson R, Carman W. During the summer 2009 outbreak of "swine flu" in Scotland what respiratory pathogens were diagnosed as H1N1/2009? BMC Infect Dis. 2011;11:1–7.

[27] Pascalis H, Temmam S, et al MTM. Intense Co-Circulation of Non-Influenza Respiratory Viruses during the First Wave of Pandemic Influenza pH1N1/2009: A Cohort Study in Reunion Island. PLoS ONE. 2012;7:e44755.

[28] Suzuki A, Camacho A, Ariyoshi K. Potential effect of virus interference on influenza vaccine effectiveness estimates in test-negative designs. Epidemiol Infect. 2014;142:2642–2646.

[29] Nickbakhsh S, Thorburn F, Wissmann BV, McMenamin J, Gunson R, Murcia P. Extensive multiplex PCR diagnostics reveal new insights into the epidemiology of viral respiratory infections. Epidemiol Infect. 2016;144:2064–2076.

[30] Lawson A. Bayesian Disease Mapping Hierarchical Modeling in Spatial Epidemiology. Boca Raton: Chapman & Hall/CRC; 2009.

[31] Knorr-Held L, Hohle M, Hofmann M. A statistical framework for the analysis of multivariate infectious disease surveillance data. Stat Modelling. 2005;5:187–199.

[32] Kleinman K, Lazarus R, Platt R. A generalized linear mixed models approach for detecting incident clusters of disease in small areas, with an application to biological terrorism. Am J Epidemiol. 2004;159:217–224.

[33] Oliveira VD. Bayesian analysis of conditional autoregressive models. Ann Inst Stat Math. 2012;64:107–133.

[34] MacNab Y. On identification in Bayesian disease mapping and ecological-spatial regression models. Stat Methods Med Res. 2014;23:134–155.

[35] Jin X, Carlin B, Banerjee S. Generalized Hierarchical Multivariate CAR Models for Areal Data. Biometrics. 2005;61:950–961.

[36] Chen Z, Dunson D. Random Effects Selection in Linear Mixed Models. Biometrics. 2003;59:762–769.

[37] Pourahmadi M. Covariance Estimation: The GLM and Regularization Perspectives. Stat Sci. 2011;26:369–387.

[38] Kruschke J. Doing Bayesian Data Analysis. 2nd ed. Amsterdam: Academic Press; 2001.

[39] Plummer M. JAGS: A program for analysis of Bayesian graphical models using Gibbs sampling; 2003. .

[40] Su Y, Yajima M. R2jags: A Pacakge for Running 'JAGS' from R; 2015.

[41] R Core Team. R: A Language and Environment for Statistical Computing. Vienna, Austria; 2015.

[42] Benjamini Y, Hochberg Y. Controlling the false discovery rate: a practical and powerful approach to multiple testing. J R Stat Soc Series B Stat Methodol. 1995;57:289300.

[43] Casalegno J, Ottmann M, Duchamp MB, Escuret V, Billaud G, Frober E, et al. Rhinoviruses delayed the circulation of the pandemic influenze A (H1N1) 2009 virus in France. Eur J Clin Microbiol Infect Dis. 2010;16:326–329.